Published in final edited form as:
Sci Transl Med. 2014 January 22; 6(220): 220ra10. doi:10.1126/scitranslmed.3007523.

Gene Therapy Prolongs Survival and Restores Function in Murine and Canine Models of Myotubular Myopathy

Martin K Childers[1,2,†], **Romain Joubert**[3], **Karine Poulard**[3], **Christelle Moal**[3], **Robert W Grange**[4], **Jonathan A Doering**[4], **Michael W Lawlor**[5,6], **Branden E. Rider**[5], **Thibaud Jamet**[3], **Nathalie Danièle**[3], **Samia Martin**[3], **Christel Rivière**[3], **Thomas Soker**[6], **Caroline Hammer**[3], **Laetitia Van Wittenberghe**[3], **Mandy Lockard**[7], **Xuan Guan**[7], **Melissa Goddard**[7], **Erin Mitchell**[7], **Jane Barber**[7], **J. Koudy Williams**[7], **David L Mack**[1], **Mark E Furth**[8], **Alban Vignaud**[3], **Carole Masurier**[3], **Fulvio Mavilio**[3], **Philippe Moullier**[3,9,10], **Alan H Beggs**[5,†], and **Anna Buj-Bello**[3,†]

[1]Department of Rehabilitation Medicine, School of Medicine, University of Washington;

[2]Institute for Stem Cell and Regenerative Medicine, University of Washington, Campus Box 358056, Seattle, WA 98109, USA

[3]Généthon, INSERM, 1 bis rue de l'Internationale, 91002 Evry, France

[4]Department of Human Nutrition, Foods and Exercise, Virginia Polytechnic Institute and State University, Blacksburg, VA 24061, USA

[5]The Manton Center for Orphan Disease Research, Children's Hospital Boston, Harvard Medical School, 300 Longwood Ave, Boston, MA 02115, USA

[6]Department of Pathology and Laboratory Medicine, Children's Hospital and Medical College of Wisconsin, Milwaukee, WI, USA

[7]Wake Forest Institute for Regenerative Medicine, 391 Technology Way, Winston-Salem, NC 27101, USA

[8]Comprehensive Cancer Center, Wake Forest University Health Sciences, School of Medicine, Medical Center Boulevard, Winston-Salem, NC 27157, USA

[9]INSERM U649, Atlantic Gene Therapies, CHU Hôtel Dieu, 44300 Nantes, France

[10]Molecular Genetics and Microbiology Department, University of Florida, Gainesville, FL 32611, USA

[†]To whom correspondence should be addressed. abujbello@genethon.fr (A.B.B); beggs@enders.tch.harvard.edu (A.H.B.); mkc8@uw.edu (M.K.C).

Author contributions: M.K.C., M.E.F., R.W.G., M.W.L., CM., F.M., P.M., A.H.B., and ABB. participated in the study design. For the canine studies, M.K.C., M.N.H., R.W.G., X.G., M.G. and E.M. carried out physiological assays, T.S., K.P. and J.D analyzed image and/or myograph data, M.W.L. performed histolopathological studies, E.M. and J.B. provided breeding and animal care oversight, K.P. and CM performed vector biodistribution, immunoblots, immunohistochemistry, and other immunological assays. R.J., Ch.M., T.J., K.P., N.D., C.H. and L.V.W performed mouse studies. S.M., CR. produced AAV vectors. M.K.C, R.W.G., M.W.L., A.V., CM., F.M., P.M., A.H.B., and A.B.B. reviewed some or all of the primary data. M.K.C, M.E.F., F.M. and A.B.B. wrote the manuscript. All authors reviewed the manuscript.

Competing interests: The authors declare that they have no competing interests.

Abstract

Loss-of-function mutations in the myotubularin gene (*MTM1*) cause X-linked myotubular myopathy (XLMTM), a fatal, congenital pediatric disease that affects the entire skeletal musculature. Systemic administration of a single dose of a recombinant serotype-8 adeno-associated virus (AAV8) vector expressing murine myotubularin to *Mtm1*-deficient knockout mice at the onset or at late stages of the disease resulted in robust improvement in motor activity and contractile force, corrected muscle pathology and prolonged survival throughout a 6-month study. Similarly, single-dose intravascular delivery of a canine AAV8-*MTM1* vector in XLMTM dogs markedly improved severe muscle weakness and respiratory impairment, and prolonged lifespan to more than one year in the absence of toxicity, humoral and cell-mediated immune response. These results demonstrate the therapeutic efficacy of AAV-mediated gene therapy for myotubular myopathy in small and large animal models, and provide proof of concept for future clinical trials in XLMTM patients.

INTRODUCTION

Seminal clinical studies have recently shown that gene replacement therapy based on localized or systemic administration of adeno-associated viral (AAV) vectors has significant potential for the treatment of human monogenic diseases, such as retinal degeneration, metabolic disorders or hemophilia (1–4). AAV vectors are excellent candidates to also treat neuromuscular diseases, however to date, trials in patients with muscular dystrophies have been limited to local intramuscular injections with no obvious clinical benefit (5–8)

X-linked myotubular myopathy (XLMTM; OMIM 310400) is a fatal non-dystrophic disease of skeletal muscle that affects approximately one in 50,000 male births. Patients typically present marked hypotonia, generalized muscle weakness and respiratory failure at birth (9). Survival beyond the postnatal period requires intensive support, often including gastrostomy feeding and mechanical ventilation. XLMTM results from loss-of-function mutations in the Myotubularin 1 gene (*MTM1*) (10), which encodes the founder of a family of 3-phosphoinositide phosphatases acting on the second messengers phosphatidylinositol 3-monophosphate [PI(3)P] and phosphatidylinositol 3,5-bisphosphate [$PI(3,5)P_2$] (11, 12). Although myotubularin is expressed ubiquitously, loss of this enzyme primarily affects skeletal muscles. Myogenesis occurs, but muscle fibers throughout the body are hypotrophic and display structural abnormalities, with associated weakness (13). No effective therapy exists for XLMTM.

Animal models of the disease currently exist in zebrafish, mouse and dog (13–15). Genetic disruption of *Mtm1* in mice causes profound abnormalities in skeletal muscle mass, structure and function, regardless of whether expression is knocked out constitutively or only in a muscle-specific fashion (13, 16). The murine phenotype resembles human XLMTM, with similar pathology and early mortality. Local injection of an *Mtm1* AAV vector rescued muscle function in the muscle-specific knockout model, indicating that restoration of functional myotubularin could ameliorate the disease phenotype (17). In the canine model - Labrador retrievers carrying an X-linked *MTM1* missense mutation - muscles from affected males exhibit strongly reduced synthesis and altered localization of myotubularin, likely due

to sequestration and degradation of the misfolded protein. The clinical picture closely resembles that of patients with comparably severe mutations, and survival does not normally exceed four months (15).

Here, we report two studies showing the long-term therapeutic potential of systemic administration of an AAV8 vector expressing the myotubularin gene under the control of a muscle-specific promoter in the murine and canine models of XLMTM. In *Mtm1*-deficient mice, tail-vein injection of AAV8-*Mtm1* at a dose of 10^{13} vector genomes per kilogram (vg/kg) at onset or at later stages of the disease corrected muscle pathology and prolonged survival throughout the six-month study. In 9-week-old *MTM1*-deficient dogs, intravascular administration of AAV8-*MTM1* at the same dose was well tolerated, rescued the skeletal muscle pathology and respiratory function, and prolonged life for over one year. Together these studies show the feasibility, safety and efficacy of gene therapy with AAV8 for long-term correction of impairment seen in these myotubularin-deficient mouse and dog models, and open the way to clinical trials aimed at correcting this devastating disease.

RESULTS

Systemic *Mtm1* delivery restores growth and survival of *Mtm1* knock-out mice

Myotubularin knock-out mice (*Mtm1* KO) display muscle pathology by 3 weeks of age (Fig. S1) and survive on average less than 2 months, as previously described (13, 18). To correct the MTM1 deficiency, we developed a muscle-tropic serotype-8 AAV vector expressing the *Mtm1* cDNA under the control of a muscle-specific desmin promoter (AAV2/8-pDesmin-*Mtm1*, abbreviated AAV8-*Mtm1*). The vector was produced in HEK293 cells by a tri-transfection-based system, formulated for *in vivo* injection, and used to treat two groups of KO mice at different stages of disease evolution, at the early onset of the pathology (3 weeks-of-age) or at the late stage of the disease, when mortality occurs (5 weeks-of-age). A single tail-vein injection of AAV8-*Mtm1* at a dose of 3×10^{13} vg/kg in *Mtm1* KO mice at 3 weeks (KO Early; n = 8) conferred long-term survival and nearly normal growth parameters to 100% of the treated animals (Fig. 1A, movie S1). The same dose was administered to severely affected mice at 5 weeks (KO Late; n =11), when 20% of the animals had already died. All treated mice remained viable and gained body mass over a 6-month observation period, except for a single 5-week-old mouse that died one day after injection (Fig. 1, B and C). Consistent with their robust appearance, skeletal muscles grew to normal size in vector-injected *Mtm1* KO mice. In both the early- and late-treated cohorts, each of the seven individual muscles analyzed gained mass, reaching >70% of WT mass at 6 months (Fig. 1D).

Analysis of myotubularin expression by Western blotting in individual muscles at sacrifice demonstrated that intravenous delivery of AAV8-*Mtm1* reconstituted efficient myotubularin synthesis in skeletal muscles throughout the body. Myotubularin levels ranged between 1- and 5-fold WT values in most skeletal muscles with no major differences between the two cohorts, except for two peaks of >15-fold expression in the *soleus* (SOL) muscle of early-treated KO mice and of >40-fold in the *tibialis anterior* (TA) of late-treated KO mice (Fig. 1E). Myotubularin was highly overexpressed in the heart (720±153 times the endogenous level 6 months after treatment). The AAV8-*Mtm1* average vector copy number (VCN,

corresponding to viral genomes / diploid genome) in early- and late-treated mice was 0.72±0.1 and 0.87±0.1 in the *tibialis anterior* and 1.67±0.4 and 3.33±2.1 in the *biceps brachii* (BI) muscle, respectively. Vector copy number in the heart and liver ranged between 1.17-5.14 and 80–223 respectively, consistent with the known tropism of AAV8. At necropsy, the heart of AAV-treated KO mice showed the presence of some focal lesions with scar tissue and a modest cellular infiltrate, although these lesions did not affect survival in any of the treated mutant animals.

Mtm1 gene therapy corrects muscle pathology and function in myotubularin-deficient mice

The muscles of *Mtm1* KO mice treated with AAV8-*Mtm1* underwent sustained amelioration of pathological features. Fig. 2 shows representative histology from the TA and BI limb muscles of untreated, 5-week-old *Mtm1* KO mice and AAV-treated, 6-month-old KO mice, demonstrating normalized cross-sectional fiber size and intracellular architecture, as revealed by hematoxylin-eosin (HE) and NADH-tetrazolium reductase (NADH-TR) staining (see Fig. S2 for additional information). Morphometry of TA and BI myofibers from 5-week-old *Mtm1* KO mice gave a mean diameter of 15.9± 0.8 μm and 17±0.7 μm respectively, with many fibers below 20 μm, compared to 28.7±0.8 μm and 24.3±1.2 μm for WT mice (Fig. 2B and Fig. S2A). Six months after treatment with AAV8-*Mtm1*, the abundance of extremely small-diameter myofibers was eliminated, and the size distribution approached that of WT muscles in both cohorts. In addition, myofibers of treated mice displayed a reduced frequency of centrally localized nuclei, a diagnostic feature of centronuclear myopathies like XLMTM (Fig. S2B).

Distinctive features of myotubularin-deficient myofibers include aberrant accumulations of mitochondria (13) and a marked deficiency of transverse tubules (T-tubules), invaginations of the plasma membrane perpendicular to the length of the myofiber that are critical for excitation-contraction coupling and muscle function (14, 18). Untreated *Mtm1* KO mice showed abnormal localization of proteins associated with the T-tubule system, including the dihydropyridine 1α receptor (DHPR1α), a voltage-gated Ca channel, and dysferlin, a transmembrane protein involved in Ca-dependent membrane repair (Fig. 2A). Treatment with AAV8-*Mtm1* corrected abnormal mitochondria distribution and cellular mislocalization of DHPR1α and dysferlin in all mice from both cohorts, indicating that XLMTM-associated pathology can be reversed well after the onset of the disease.

Structural muscle abnormalities are mirrored by severe functional deficits in *Mtm1* KO mice. To measure the effect of gene therapy on muscle function, the open-field actimeter, global muscle strength, and isolated limb strength assays were used. Open-field actimeter measurements showed that mutant mice covered less than half the distance explored by WT mice at 5 weeks of age (Fig. 3A). Mice treated with AAV8-*Mtm1* at both early and late stages of the disease showed significant functional improvement, and at 6 months post-AAV injection their motor activity was indistinguishable from that of WT animals. A non-invasive test of global muscle strength that measures forward pulling tension in an escape paradigm revealed that untreated *Mtm1*-deficient mice were half as strong as WT mice (whole body tension, 0.07±0.01 *vs*. 0.15±0.01 N/g) (Fig. 3B). Early- and late-treated mice showed 82% (0.15±0.01 N/g) and 76% (0.13 ± 0.01 N/g) recovery of whole body tension, respectively

(Fig. 3B). In a functional assay of an isolated hind limb muscle, the *extensor digitorum longus* (EDL), the isometric force of untreated *Mtm1* KO mice was only 13% of the WT level, while it almost normalized 6 months after AAV8-*Mtm1* delivery in both cohorts (Fig. 3C). Together, these data indicate that muscle impairment associated with myotubularin deficiency can be rescued by gene therapy even after the onset of pathology.

Correction of muscle pathology in myotubularin-deficient mice is dose-dependent

To assess the effect of a lower vector dose on phenotype correction, 5×10^{12} vg/kg of AAV8-*Mtm1* were injected into the tail vein of *Mtm1* KO mice at 3 weeks of age (n = 10). This dose prolonged the survival of 50 % of the mice over 3 months, with the first death occurring 6 weeks after injection (Fig. S3A). Body weight increased during the first 3 weeks of treatment and remained unchanged after this period (Fig. S3B). This partial recovery of body mass was reflected at the level of individual skeletal muscles: two of the 7 analyzed muscles (*soleus* and *biceps brachii*) grew normally, while the other 5 reached 40 to 60% of WT mass at 3 months (Fig. S3C). The motor activity of mice treated with the low vector dose appeared indistinguishable from that of WT mice and KO mice treated with the high dose in an open-field actimeter assay 3 months post-injection (Fig. S3E). However, their global muscle strength was reduced by 55 % in the more sensitive escape test, and their isolated *soleus* and EDL muscles generated 60% and 9% of the WT force, respectively, indicating that muscle function recovery was not complete in the low dose cohort. In the EDL, only 3% of myotubularin endogenous level was reached (Fig. S3D), ranging from 7% to 27 % in the other analyzed muscles (mean = 13%), indicating that low levels of MTM1 are sufficient to prolong the survival of mutant mice.

Intramuscular injection of AAV8-*MTM1* ameliorates pathology and increases strength of myotubularin-deficient canine muscles

To evaluate myotubularin gene replacement therapy in a large animal model, we studied male XLMTM Labrador/Beagle F1 offspring, which display the same pathology and clinical features of the previously reported XLMTM pure-bred Labradors (15). These dogs become symptomatic by 9–10 weeks of age and muscular weakness progresses up to ~18 weeks of age, when animals can no longer ambulate and rapidly die. For this study, we generated a recombinant AAV8 vector carrying the canine *MTM1* cDNA under the control of the desmin promoter, as in the murine vector (AAV2/8-pDesmin-*MTM1* or AAV8-*MTM1*). The vector was produced in SF9 cells by a baculovirus-based system, purified by affinity chromatography and formulated for *in vivo* injection. To assess transgene expression and the local effect on diseased muscle, a single dose of 4×10^{11} vg of the AAV8-*MTM1* vector was injected into the middle part of the *cranial tibialis* hind limb muscle of XLMTM dogs at 10 weeks of age (n=3). The contralateral muscles received only saline. Dogs were sacrificed after 4–6 weeks and injected muscles analyzed for histological appearance, protein expression and function. All AAV-treated muscles grew in mass and volume by about 50% compared to the contralateral, saline-injected muscles, as shown by weight/volume measurements and computer tomography (CT) scans (Fig. 4A and Fig. S4). AAV-injected muscles consistently showed improved architecture, with increased myofiber size, normalization of mitochondria positioning and cellular localization of DHPR1α and dysferlin (Fig. 4C). Electron microscopy confirmed that, compared to WT muscle, XLMTM

muscle contained few characteristic T-tubules but showed atypical longitudinal structures (L-tubules). By contrast, AAV8-*MTM1*-injected mutant muscles closely resembled WT, with abundant T-tubules (Fig. 4C, Supplementary Table S1). Expression of vector-driven MTM1 protein was analyzed on whole muscle lysates by Western blotting using an antibody against canine myotubularin. Immunoblot analysis showed substantial myotubularin expression in the injected muscles of all treated dogs (Fig. 4A), decreasing from approximately 60% of the WT levels at the center of the *cranial tibialis* to about 8% at its ends. Some myotubularin expression was detected in the contiguous EDL muscles, while no expression was detected in the contralateral limb muscles nor in distant muscles such as the diaphragm or the heart.

To evaluate the effect of treatment on muscle function, we used force transduction assays developed to assess the strength of the distal part of canine hind limbs during flexion, mainly generated by the *cranial tibialis* muscle (Fig. 4B depicts an isometric contraction assay) (19–21). Immediately prior to gene therapy at 10 weeks of age (baseline), XLMTM dogs were slightly weaker than unaffected WT littermates, and the two hind limbs of each dog performed equally (Fig. 4B). Measurements of force 4 and 6 weeks later showed more than doubled limb strength in WT dogs, consistent with normal muscular maturation. In mutant dogs, the strength of AAV8-*MTM1*-treated limbs increased strikingly already 4 weeks after injection and reached 80% of WT force at 6 weeks, whereas limbs injected with saline did not improve. We also used a dynamic eccentric contraction assay to measure muscular performance over prolonged exercise (Fig. S5). When assessed by this test, the hind limbs of young WT dogs strengthened over time, while saline-injected limbs of all three XLMTM dogs declined to about 20% of WT values. Again, injection of AAV8-*MTM1* greatly improved muscle performance: at 14 and 16 weeks-of-age, treated limbs achieved >70% of WT strength (Fig. S5, B–D). These results showed that a single injection of AAV8-*MTM1* is efficacious in rescuing the function of an entire myotubularin-deficient muscle, prompting us to assess an intravascular delivery approach.

Intravascular administration of AAV8-*MTM1* rescues muscle pathology and prolongs survival of XLMTM dogs

AAV delivery by isolated limb perfusion allows widespread transduction of muscle groups in dogs and non-human primates (22–24). To test whether regional administration is sufficient to ameliorate muscle pathology in an entire limb, we injected a single dose of 2.5×10^{13} vg/kg of AAV8-*MTM1* under high pressure into the saphenous vein of three 9-wk-old XLMTM dogs, after applying a tourniquet around the hind limb distal to the injection site to limit blood circulation during infusion. The tourniquet was released 5 minutes after injection. Treated dogs improved in strength rapidly after vector administration. In contrast to dogs injected intramuscularly, where only the muscles of the injected limb gained strength, high pressure intravascular limb delivery of AAV8-*MTM1* resulted in improved strength of both the infused and contralateral hind limbs, which reached on average almost normal values 6 weeks after infusion (Fig. 5A and Fig. S6). Similarly, peak inspiratory flow, which was strongly reduced in XLMTM dogs at 16 weeks of age, was normal in treated dogs (Fig. 5B), indicating that the AAV8-*MTM1* vector had transduced respiratory muscles and improved their function. Most importantly, all treated dogs showed a dramatic

improvement in survival, which extended far beyond the critical 18-week time point, when all untreated XLMTM dogs can no longer ambulate and need to be euthanized. The first infused XLMTM dog (Dog 4) survived in relatively good condition beyond 1 year, and was sacrificed for analysis at 14 months of age. The other two dogs (Dog 5 and Dog 6) remained ambulant and clinically robust beyond the age of 1 year, and are alive and healthy at the time of manuscript preparation (movie S2).

Muscle biopsies were taken from the injected and contralateral hind limbs (quadriceps, *biceps femoris*) and from the fore limbs (triceps, *biceps brachii*) of all treated dogs 4 weeks post-infusion to analyze vector distribution, transgene expression and histology. Intravenous administration of AAV8-*MTM1* improved myofiber appearance and architecture in the treated limbs, which consistently showed an average fiber size only slightly reduced compared to WT muscles (Fig. 6A). In contrast, non-infused limbs displayed heterogeneity in muscle fiber size, with coexistence of small and large fibers. Mislocalization of organelles was seen in biopsies from only one of the three AAV-infused XLMTM dogs (Dog 4) and was more pronounced in the non-infused limb (Fig. 6A). Electron microscopy performed on quadriceps muscle samples obtained from all infused limbs showed normalized sarcotubular organization, similar to what observed after intramuscular injection (Supplementary Table S2). The *biceps femoris* muscles of Dog 4, analyzed at sacrifice, revealed a partially defective sarcotubular organization in both the infused and non-infused hindlimb, with only approximately 1 triad per field in each muscle (Supplementary Table S3).

Western blot analysis demonstrated myotubularin expression in all muscle samples obtained from all three treated dogs (Fig. 7B): four weeks after infusions, the level of myotubularin expression reached 21 to 72 % of the WT control levels in the *biceps femoris* and quadriceps muscles in the injected limbs and 9 to 138 % in the muscles (quadriceps, *biceps femoris*, triceps, *biceps brachii*) of the non-injected limbs. Expression levels were paralleled by VCN levels, which ranged from 0.52 to 2.35 in the *biceps femoris* and quadriceps muscles of the infused limbs and from 0.17 to 3.65 in the muscles of the non-injected limbs (Figure 7B). The biodistribution of AAV8-*MTM1* was analyzed in Dog 4 at necropsy. The VCN was in general higher in infused muscles (range: 0.01–2.27) than in distal muscles (range: 0.007-0.13, n=18), with the exception of the diaphragm, intercostal muscles and heart, where we detected a VCN of 0.37, 0.59 and 0.28, respectively (Fig. 7C). MTM1 protein levels were above the endogenous level in 7 out of 13 muscles from the infused hind limb and barely detectable in the contralateral and fore limb muscles (Fig. 7D), mirroring the VCN values and suggesting that very low amounts of myotubularin are sufficient to rescue muscle function. In the diaphragm and heart, myotubularin reached 64% and 13% of the WT values, respectively. The heart of Dog 4 showed no signs of toxicity at histological examination (Fig. S7) and at the functional level, as assessed by electrocardiogram and echocardiography prior to necropsy. The histology of the liver (VCN: 0.63) was also normal, and myotubularin protein was undetectable.

These data show that isolated limb perfusion was effective in delivering the AAV vector to the infused muscle groups but did not limit vector diffusion to other organs, including the rest of the skeletal musculature and the heart.

Intramuscular or intravascular delivery of AAV8-*MTM1* elicits no humoral or cytotoxic immune response against the transgene product in XLMTM dogs

The neutralizing factor (NAF), IgG and IgM titers specific to AAV8 were measured in XLMTM dog's sera before and after intramuscular (Supplementary Fig. S8A) or intravascular (Fig. S8B) administration of AAV8-*MTM1*. NAF and IgG titers increased one week after injection and remained elevated for up to 10 months in all treated animals, while IgM titers decreased to pre-infusion levels in dogs treated by intravascular infusion. Conversely, MTM1-specific IgG or IgM antibodies remained undetectable in all treated animals (Fig. S8C and D). Cell-mediated immune responses against the vector or the transgene product were tested by an IFN-γ Elispot assay on PBMCs over a period of 155 days after vector administration. We were unable to detect any T cells specific to the vector capsid nor the MTM1 protein in XLMTM dogs given intramuscular or intravenous AAV8-MTM1 (Supplementary Fig. S9).

Inflammatory cytokines (IL2, IL6, IL8, IL10, IL15, TNF-α and IFN-γ) were profiled in XLMTM dogs before and after intramuscular or intravascular infusion of AAV8-*MTM1* (Supplementary Table S4). Of the three dogs injected intramuscularly, one (Dog 3) displayed elevated TNF-α levels (42.5–80.8 pg/ml) between day 3 and day 28 post-injection. Transient elevation of IL2 and IL15 levels (743.5 and 119 pg/ml, respectively) was observed in only one dog treated intravascularly (Dog 6) 6 hrs after infusion. No elevation of inflammatory cytokines levels was observed in the other animals, including untreated controls, throughout the observation period.

DISCUSSION

Gene therapy of neuromuscular disorders requires body-wide distribution of the therapeutic gene, and therefore systemic delivery of a gene transfer vector capable of transducing skeletal muscles and, if necessary, the heart. AAV vectors are attractive candidates due to their natural tropism for muscle and their small size, which allows access to fibers through the vascular endothelium and the basement membrane. Pre-clinical and clinical studies proved that AAV-mediated delivery can lead to transgene expression at therapeutic or sub-therapeutic levels in entire muscles, and can correct the disease phenotype in animal models of muscular dystrophy (reviewed in (25)). Clinical trials showed, however, that intramuscular injection is impractical and unlikely to provide significant clinical benefit to patients affected by limb-girdle or Duchenne muscular dystrophy (DMD) (5–8). Initial efforts aimed at targeting skeletal and cardiac muscles through intravascular delivery required the use of invasive procedures and relatively toxic permeabilizing drugs (26). However, the introduction of muscle-tropic serotypes such as AAV6, 8 and 9 allowed to transduce both skeletal and cardiac muscle by low-pressure intravascular or systemic intravenous administration, and achieve significant phenotypic correction in both murine and canine models of muscular dystrophy (27–30). Systemic AAV administration has not yet been attempted in patients.

In this study, we show long-term full phenotypic correction of MTM1-deficient myotubular myopathy in both a murine and a canine model of the disease by intravenous administration of an AAV8 vector carrying a muscle-specific MTM1 expression cassette. In mice, a single

tail vein administration of the AAV8-*Mtm1* vector either before or after the onset of the pathology achieved full rescue of the disease for the duration of the study. The fact that the MTM1 pathology could be corrected in already severely affected mice indicates that the damage induced by the absence of MTM1 is reversible, a particularly important finding in view of a clinical translation of XLMTM gene therapy, which will inevitably involve already symptomatic patients. However, differences exist between the clinical presentation of XLMTM in patients compared to animal models. In particular, patients typically present with respiratory failure at birth whereas mice and dogs develop respiratory weakness later in life. Thus, it may be necessary to develop specific clinical protocols for treating very young children and balance the risk of treatment versus that of assisted ventilation.

To confirm the therapeutic potential of the AAV8-*MTM1* vector in the XLMTM dog model, we decided to use a clinically relevant delivery method based on isolated limb perfusion. This delivery route showed feasibility and safety in a clinical trial on volunteer patients affected by several forms of muscular dystrophy (31). We intended to use high pressure intravascular hind limb administration as an intermediate approach between direct intramuscular muscle injection, which confirmed the therapeutic potential of the AAV8-*MTM1* vector even in large muscles, and full systemic administration. Surprisingly, we observed a dramatic rescue of the lethality and a systemic correction of the skeletal muscle pathology in all treated dogs throughout the duration of the one year study. Intravascular delivery of the AAV8-*MTM1* vector under pressure against a tourniquet led to efficient transduction of all muscles in the infused limb but also of distal muscles and organs, though at a lower level in terms of both VCN and protein expression. Remarkably, the respiratory muscles, and particularly the diaphragm, were well transduced and their function normalized in all animals. This is the first demonstration of complete and persistent phenotypic correction of a monogenic neuromuscular disease in a large animal model by a single intravenous administration of an AAV vector. Our results indicate that systemic intravenous administration may be the simplest and most effective way of administering an AAV-based gene therapy for XLMTM in patients, although additional dose-finding and toxicity studies will be necessary before launching a clinical trial.

The unpredicted systemic effect of the high pressure intravascular vector administration in the present study is in contrast with previous studies of tightly restricted vector transduction in the limbs of hemophilic and golden retriever muscular dystrophy (GRMD) dogs, infused with AAV1 or AAV2 vectors (24, 32). Although blood flow was monitored in the present study by ultrasound above and below the constriction during infusion, the tourniquet was apparently inefficient in limiting vector delivery to the infused limb, due to slippage, collateral circulation or other less obvious factors. The tourniquet was released after 5 minutes, when a substantial amount of vector was apparently still available to enter the systemic circulation and transduce distant organs. A longer persistence of the AAV8 with respect to an AAV1 or AAV2 vector in the isolated limb circulation might have also contributed to the ineffective restriction. The gradient of VCN distribution above and below the tourniquet was more pronounced in the first treated dog, D4, than in the subsequent two, D5 and D6, where the vector transduced almost uniformly all muscles, indicating a certain variability in the limb isolation procedure.

The quasi-systemic vector administration was well tolerated by all three XLMTM dogs, which showed no signs of acute or chronic toxicity. Liver-enzyme levels were within the range of normality in all dogs throughout the study, and the histology of D4's liver appeared to be normal at necropsy. Likewise, no toxicity was observed in the systemically treated mutant mice, with the exception of focal heart inflammatory infiltrates and fibrotic lesions detected in animals treated at the highest dose (3×10^{13} vg/kg), but otherwise asymptomatic. This was not observed in the heart of D4 at necropsy, which was completely normal one year after vector administration. The desmin promoter is very active in the cardiac muscle (33), and caused a dramatic MTM1 overexpression in murine heart. Conversely, MTM1 expression was below the endogenous level in the heart of D4, which was treated with a similarly high dose compared to the mouse study (2.5×10^{13} vg/kg) although through a different route. This suggests that accessibility from the systemic circulation, heart tropism of the AAV8 vector, or desmin promoter function may vary among different species, and indicates the need for a specific toxicity study in large animals before advancing to a clinical trial.

Our study shows that the threshold of myotubularin expression required for therapeutic benefit in XLMTM mice and dogs is well below the normal levels and may vary among different muscles, as observed for other neuromuscular disorders due to enzyme rather than structural protein deficiency (34). In *Mtm1* knockout mice, administration of low levels of an engineered myotubularin protein were sufficient to improve both muscle function and pathology (35). In other studies, mice carrying an engineered *Mtm1* missense mutation that affects RNA splicing and leaves just traces of myotubularin activity survive 8 times longer than constitutive *Mtm1* knockout mutants (36). In the present study, the amount of myotubularin present in skeletal muscles of mice six months after high-dose vector injection ranged between 1 and 5 times the endogenous levels, leading to full correction. A lower vector dose led to synthesis of 3 to 27% of the normal myotubularin levels in treated mice, which was curative for some but not all muscles but was still able to prolong survival. In dogs, the vector-derived myotubularin level in skeletal muscles was also variable, and in general higher in the infused limb. In dog D4, where differences between the infused and non-infused limbs were more pronounced, functional reconstitution was observed even in muscles where myotubularin was barely detectable and the pathology not fully corrected. In the other two dogs, D5 and D6, the levels of myotubularin were higher in all muscles (30% to 140% as measured in biopsies) and led to an objectively better phenotypic correction in the whole body. Respiratory function was normalized in all three dogs. Lower than normal levels of myotubularin are therefore sufficient to ameliorate muscle function even in the presence of incomplete restoration of the histology, and a dose of ~2×10^{13} vg/kg was fully therapeutic in both animal models of the disease. Even though comparing doses in different studies is a difficult exercise, the results of a recent clinical study on the systemic administration of an AAV8 vector expressing human factor IX in hemophilia B patients suggest that a dose in the range of 10^{13} vg/kg may be administrable to XLMTM patients, possibly in combination with transient immunosuppression (4, 37).

In contrast to previous observations in animal models of DMD (24, 38), our data demonstrate relatively long-term expression of AAV-derived myotubularin in muscles of

XLMTM mice and dogs treated with a single dose of recombinant vector. A major difference between DMD and XLMTM is that the pathology of myotubularin-deficient muscles is not *per se* associated with inflammation nor with the cycles of degeneration/regeneration typical of dystrophic muscles (13, 15, 39). In fact, the correction of pathology observed for XLMTM is unlikely to occur in the advanced stages of dystrophic myopathies like DMD, where muscle fibers degenerate and are irreversibly replaced by fat and fibrotic tissue. Of note, we observed no humoral response against MTM1 or cellular immune response against either the vector or MTM1, highlighting major differences in the vector-host interactions in the case of non-dystrophic muscle pathology. Normal skeletal myofibers are long-lived, and transgene expression can persist up to 10 years in human skeletal muscle after AAV-mediated gene transfer (40). We can therefore predict that in the absence of inflammatory, humoral or cytotoxic immune responses, vector-derived MTM1 expression could persist for many years in muscles of XLMTM patients treated by gene therapy. The presence of residual levels of myotubularin, as observed in the canine animal model, will probably be a decisive factor in limiting the risk of adverse immune reactions.

In conclusion, our results demonstrate that intravenous AAV8-mediated gene therapy leads to long-term systemic correction of XLMTM in small and large animal models at doses compatible with clinical application, and pave the way to a clinical trial of gene therapy for myotubular myopathy.

Materials and Methods

Animals

Mice were handled according to French and European legislation on animal care and experimentation and approved by the institutional ethical committee. The constitutive knockout of the myotubularin gene (KO-*Mtm1*, also named BS53d4–129pas) was described previously (13, 18). Wild-type littermate males were used as controls.

Dogs were handled according to principles outlined in the National Institutes of Health *Guide for the Care and Use of Laboratory Animals*. XLMTM dogs were described previously (15). Affected males were identified by polymerase chain reaction-based genotyping, as described. Experiments were generally conducted in an open-label, non-randomized design. For dogs, muscle function data were analyzed by an investigator (JAD) blinded to the intervention.

Construction and production of AAV8-MTM1 vectors

The recombinant adeno-associated virus vector AAV2/8-pDesmin-*Mtm1*^{murine} (designated AAV8-*Mtm1*) was constructed as follows. Murine *Mtm1* cDNA (AF073996, NCBI) was cloned downstream of the human desmin promoter in the AAV2 expression plasmid pAAV2-pDes by PCR amplification. Pseudo-typed recombinant AAV2/8 viral preparations were generated by packaging AAV2-inverted terminal repeat (ITR) recombinant genomes into AAV8 capsids using a tri-transfection protocol as previously described (17). Viral titers were quantified by a TaqMan real-time PCR assay (Applied Biosystem) and expressed as viral genomes per mL (vg/mL). The recombinant adeno-associated virus vector AAV2/8-

pDesmin-*MTM1*^{canine} containing a canine myotubularin cDNA regulated by the desmin promoter (designated AAV8-c*MTM1*) was produced in a baculovirus/Sf9 system (41). Two baculovirus batches were generated, one expressing *rep* and *cap* AAV genes and the second bearing the canine *MTM1* cDNA (XM850116, NCBI) downstream from the human desmin promoter. The AAV8-c*MTM1* vector particles were produced after baculoviral double infection of insect Sf9 cells and purified from total cell culture using AVB affinity chromatography column (GE Healthcare, AVB Sepharose high performance). The concentration in vg/mL was determined from DNase-resistant particles by a TaqMan realtime PCR assay (Applied Biosystem). Other routine quality control assays for recombinant AAV vectors were performed, including sterility and purity tests.

Administration of AAV8-MTM1 vectors

Systemic vector administration in mice—AAV8-*Mtm1* at 3×10^{13} viral genomes per kg body mass (vg/kg) was injected into the tail vein of 3 and 5 week-old KO-*Mtm1* mice. An equivalent volume of saline was administrated to either KO-*Mtm1* or WT animals as controls.

Intramuscular delivery in dogs—AAV8-c*MTM1* (4×10^{11} vg) diluted in 1 ml lactated Ringer's solution was injected under ultrasound guidance into the midbelly of the cranial tibialis muscle of one hind limb of unvaccinated 10 weeks of age affected male XLMTM dogs under anesthesia. The cranial tibialis muscle of the contralateral limb was injected with an equal volume of Ringer's solution alone. Unaffected male littermates (WT) received 1 ml of Ringer's solution in each hind limb.

High pressure intravascular limb infusion—In anesthetized XLMTM dogs, AAV8-c*MTM1* (2.5×10^{13} vg/kg) diluted in phosphate buffered saline (PBS) was infused into the distal saphenous vein under pressure (300 torr) against a tourniquet as described (42). Briefly, a tourniquet was positioned at the level of the groin and adjusted until the femoral pulse was no longer detectable by ultrasound, to transiently block blood inflow to the target limb. Vector was suspended in PBS at 20% of the total hind limb volume (determined by water volume displacement) and administered via a 14 gauge catheter placed into a distal branch of the peripheral saphenous vein on the dorsum of the paw. The tourniquet was tightened for a total of 15 minutes (10 minutes prior to and 5 minutes during the infusion). In each dog, one hind limb was infused with vector whereas the contralateral hind limb was not infused. For vector copy and immunoblot analysis, the mid-section of the muscle belly was sampled at biopsy or necropsy.

Vector copy number analysis

The number of vector genomes per diploid genome was quantified from 80 ng of total DNA by Taqman real-time PCR using a 7900 HT thermocycler (Applied Biosystem, France). The canine β glucuronidase gene was used for standardization. Primers used for vector genome (*MTM1*) amplification were: *5′- ATAAGTTTTGGACATAAGTTTGC -3′*(forward), *5′-CATTTGCCATACACAATCAA -3′*(reverse) and *5′-CGACGCTGACCGGTCTCCTA -3′* (probe). Primers and probe used for β glucuronidase amplification were: *5′-*

ACGCTGATTGCTCACACCAA-3′(forward), *5′-CCCCAGGTCTGCTTCATAGTTG-3′* (reverse) and *5′-CCCGGCCCGTGACCTTTGTGA-3′*(probe) (Applied Biosystem).

Quantitative immunoblot analysis

Several muscle cryo-sections of 30 μm each (300 μm to 1 mm in total) were sliced and proteins were extracted and analyzed by sodium dodecyl sulfate-polyacrylamide gel electrophoresis and western blotting as previously described (16). Membranes were probed with either a polyclonal antibody against the C-terminal part of murine myotubularin (R2348 (17)) or a rabbit polyclonal antibody raised against the C-terminus of canine myotubularin (R1040, Généthon). A mouse monoclonal antibody specific for GAPDH (Millipore, MAB374) was used as internal control. Detection was performed with a secondary antibody coupled to IRDye 680 (*LI-COR*) and the Odyssey infrared imaging system (*LI-COR* Biotechnology Inc.).

Histological and immunofluorescence analyses

Histology and morphometry—For mouse studies, cryo-sections (7 μm) of frozen muscles were processed for hematoxylin and eosin (HE) and NADH-TR stainings using standard procedures. The proportion of internalized nuclei and the diameter of myofibers were quantified as previously described (16). For canine studies, serial 8 μm thick transverse cryo-sections were prepared from frozen muscles and processed for hematoxylin and eosin (HE) and NADH-TR stainings. The number of centrally nucleated fibers, and fibers with mislocalization of organelles (including mitochondrial aggregates and necklace fibers) were quantified manually from photographs taken at 200x magnification. For fiber size quantification, muscles were immunostained as described above with rabbit anti-dystrophin antibodies (Abcam PLC, ab15277) and AlexaFluor-conjugated anti-rabbit IgG (Molecular Probes). Staining was evaluated and MinFeret diameters of fibers were quantified using a Nikon Eclipse 90i microscope using NIS-Elements AR software (Nikon Instruments Inc.) and a BX53 microscope and CellSens Standard software (Olympus). Slides for evaluation of canine cardiac pathology were produced through the Children's Research Institute Histology Core Facility at MCW. Electron microscopy was performed at MCW's Electron Microscopy Core Facility and quantification of sarcotubular structures was performed as described previously (35).

Immunofluorescence—For immunostaining of muscle tissue, frozen transverse sections were fixed for 10 min by incubation in PBS at 100°C. Non-specific antigens were blocked with PBS, 0.2% Tween, 3% BSA at RT. Sections were then incubated at 4°C overnight with mouse primary antibodies directed against DHPR1α (Thermo Scientific Pierce, MA3–920) or Dysferlin (Novocastra, NCL-HAMLET). After extensive PBS washes, sections were incubated with biotinylated goat anti mouse antibodies (SouthernBiotech) and, after additional washes, with streptavidin conjugated with Alexa Fluor 488 (Invitrogen). Glass slides were mounted with FluorSave reagent™ (Calbiochem®, Merck) and visualized with a Leica confocal microscope TCS-SP2. Digital images of a slice corresponding to the muscle midsection were acquired with a CCD camera (Sony) and a motorized stage.

Muscle function

Muscle function in mice—Actimeter test: spontaneous locomotor activity in mice was assessed using the LE 8811 IR motor activity monitor (Bioseb). Briefly, mice were placed in an open field bounded with 16 horizontal photoelectric Infra Red beams to measure three-dimensional movements of the animals. The distance crossed was recorded and analyzed for 90 minutes. Escape test: global strength of mice was evaluated as previously described (43). Measurements of isometric contractile properties of murine EDL muscles were performed *in vitro* as published (17).

Hind limb contraction in dogs—Contractile properties in canine muscles *in vivo* were assessed as previously described (19, 20). Briefly, the hind limb torque of anesthetized dogs was measured by wrapping the foot to a pedal mounted on the shaft of a servomotor that also functioned as a force transducer. Percutaneous stimulation of the peroneal nerve activated hind limb muscles to pull the foot up toward the body to generate torque. Isometric contractions were performed over a range of stimulation frequencies to determine torque-frequency relationships and investigators blinded to the experimental treatment analyzed data.

Diaphragm muscle function in dogs—Peak inspiratory flow (PIF) was assessed under anesthesia by pneumatography as previously described (44). Briefly, airflow was measured prior to the administration of the centrally-acting stimulant doxapram chloride (1.0mg/kg) and again after respiratory increase. Raw tracings were visually examined to ensure complete capture of each breath before computer analysis. 10 clear and successive breaths were selected from those collected at baseline and again at the respiratory peak.

Statistical analysis

Statistical analyses were performed using SAS software (Version 6; SAS Institute Inc, Cary, NC). Individual means were compared using non-parametric tests (Mann-Whitney, or Wilcoxin rank-sum tests). Differences were considered to be statistically significant at either $P < 0.05$ (1 symbol) or $P < 0.01$ (2 symbols). All data are presented as means ± Standard Error of the Mean (SEM) unless stated otherwise.

Supplementary Material

Refer to Web version on PubMed Central for supplementary material.

Acknowledgments

We thank F. Barnay-Toutain, Y. Garnier, B. Gjata, M. Holder, J. Marchant, A. Menuet, K. Pappante, T. Savic, D. Stockholm, J. Tan, and P. Veron for help with the experiments; K. Block and M. Lockard for clinical support. A. Atala, C. Le Guiner and J-L. Mandel for support and/or discussions.

Funding: Association Française contre les Myopathies (AFM, France), Myotubular Trust (UK), Genopole d'Evry (France), Région d'Alsace (France), Muscular Dystrophy Association (MDA, US), US National Institutes of Health (Grants NIH P50 NS040828, R01 AR044345, K08 AR059750, R21 AR064503, R01 HL115001), Anderson Family Foundation and Joshua Frase Foundation.

References

1. Maguire AM, et al. Safety and efficacy of gene transfer for Leber's congenital amaurosis. N Engl J Med. May 22.2008 358:2240. [PubMed: 18441370]
2. Bainbridge JW, et al. Effect of gene therapy on visual function in Leber's congenital amaurosis. N Engl J Med. May 22.2008 358:2231. [PubMed: 18441371]
3. Bennett J, et al. AAV2 gene therapy readministration in three adults with congenital blindness. Sci Transl Med. Feb 8.2012 4:120ra15.
4. Nathwani AC, et al. Adenovirus-associated virus vector-mediated gene transfer in hemophilia B. N Engl J Med. Dec 22.2011 365:2357. [PubMed: 22149959]
5. Mendell JR, et al. Sustained alpha-sarcoglycan gene expression after gene transfer in limb-girdle muscular dystrophy type 2D. Ann Neurol. Nov.2010 68:629. [PubMed: 21031578]
6. Mendell JR, et al. Dystrophin immunity in Duchenne's muscular dystrophy. N Engl J Med. Oct 7.2010 363:1429. [PubMed: 20925545]
7. Herson S, et al. A phase I trial of adeno-associated virus serotype 1-gamma-sarcoglycan gene therapy for limb girdle muscular dystrophy type 2C. Brain. Feb.2012 135:483. [PubMed: 22240777]
8. Bowles DE, et al. Phase 1 gene therapy for Duchenne muscular dystrophy using a translational optimized AAV vector. Mol Ther. Feb.2012 20:443. [PubMed: 22068425]
9. Jungbluth H, Wallgren-Pettersson C, Laporte J. Centronuclear (myotubular) myopathy. Orphanet J Rare Dis. 2008; 3:26. [PubMed: 18817572]
10. Laporte J, et al. A gene mutated in X-linked myotubular myopathy defines a new putative tyrosine phosphatase family conserved in yeast. Nat Genet. Jun.1996 13:175. [PubMed: 8640223]
11. Laporte J, et al. Characterization of the myotubularin dual specificity phosphatase gene family from yeast to human. Hum Mol Genet. Oct.1998 7:1703. [PubMed: 9736772]
12. Robinson FL, Dixon JE. Myotubularin phosphatases: policing 3-phosphoinositides. Trends Cell Biol. Aug.2006 16:403. [PubMed: 16828287]
13. Buj-Bello A, et al. The lipid phosphatase myotubularin is essential for skeletal muscle maintenance but not for myogenesis in mice. Proc Natl Acad Sci U S A. Nov 12.2002 99:15060. [PubMed: 12391329]
14. Dowling JJ, et al. Loss of myotubularin function results in T-tubule disorganization in zebrafish and human myotubular myopathy. PLoS Genet. Feb.2009 5:e1000372. [PubMed: 19197364]
15. Beggs AH, et al. MTM1 mutation associated with X-linked myotubular myopathy in Labrador Retrievers. Proc Natl Acad Sci U S A. Aug 17.2010 107:14697. [PubMed: 20682747]
16. Joubert R, et al. Site-specific Mtm1 mutagenesis by an AAV-Cre vector reveals that myotubularin is essential in adult muscle. Hum Mol Genet. May 1.2013 22:1856. [PubMed: 23390130]
17. Buj-Bello A, et al. AAV-mediated intramuscular delivery of myotubularin corrects the myotubular myopathy phenotype in targeted murine muscle and suggests a function in plasma membrane homeostasis. Hum Mol Genet. Jul 15.2008 17:2132. [PubMed: 18434328]
18. Al-Qusairi L, et al. T-tubule disorganization and defective excitation-contraction coupling in muscle fibers lacking myotubularin lipid phosphatase. Proc Natl Acad Sci U S A. Nov 3.2009 106:18763. [PubMed: 19846786]
19. Kornegay JN, et al. Contraction force generated by tarsal joint flexion and extension in dogs with golden retriever muscular dystrophy. J Neurol Sci. Jul 1.1999 166:115. [PubMed: 10475104]
20. Childers MK, Grange RW, Kornegay JN. In vivo canine muscle function assay. J Vis Exp. 2011
21. Grange RW, et al. Muscle function in a canine model of X-linked myotubular myopathy. Muscle Nerve. Oct.2012 46:588. [PubMed: 22987702]
22. Su LT, et al. Uniform scale-independent gene transfer to striated muscle after transvenular extravasation of vector. Circulation. Sep 20.2005 112:1780. [PubMed: 16157771]
23. Toromanoff A, et al. Safety and efficacy of regional intravenous (r.i.) versus intramuscular (i.m.) delivery of rAAV1 and rAAV8 to nonhuman primate skeletal muscle. Mol Ther. Jul.2008 16:1291. [PubMed: 18461055]
24. Vulin A, et al. Muscle function recovery in golden retriever muscular dystrophy after AAV1-U7 exon skipping. Mol Ther. Nov.2012 20:2120. [PubMed: 22968479]

25. Goyenvalle A, Seto JT, Davies KE, Chamberlain J. Therapeutic approaches to muscular dystrophy. Hum Mol Genet. Apr 15.2011 20:R69. [PubMed: 21436158]
26. Greelish JP, et al. Stable restoration of the sarcoglycan complex in dystrophic muscle perfused with histamine and a recombinant adeno-associated viral vector. Nat Med. Apr.1999 5:439. [PubMed: 10202936]
27. Gregorevic P, et al. Systemic delivery of genes to striated muscles using adeno-associated viral vectors. Nat Med. Aug.2004 10:828. [PubMed: 15273747]
28. Gregorevic P, Blankinship MJ, Allen JM, Chamberlain JS. Systemic microdystrophin gene delivery improves skeletal muscle structure and function in old dystrophic mdx mice. Mol Ther. Apr.2008 16:657. [PubMed: 18334986]
29. Inagaki K, et al. Robust systemic transduction with AAV9 vectors in mice: efficient global cardiac gene transfer superior to that of AAV8. Mol Ther. Jul.2006 14:45. [PubMed: 16713360]
30. Wang Z, et al. Successful regional delivery and long-term expression of a dystrophin gene in canine muscular dystrophy: a preclinical model for human therapies. Mol Ther. Aug.2012 20:1501. [PubMed: 22692496]
31. Fan Z, et al. Safety and feasibility of high-pressure transvenous limb perfusion with 0.9% saline in human muscular dystrophy. Mol Ther. Feb.2012 20:456. [PubMed: 21772257]
32. Arruda VR, et al. Peripheral transvenular delivery of adeno-associated viral vectors to skeletal muscle as a novel therapy for hemophilia B. Blood. Jun 10.2010 115:4678. [PubMed: 20335222]
33. Li Z, Colucci E, Babinet C, Paulin D. The human desmin gene: a specific regulatory programme in skeletal muscle both in vitro and in transgenic mice. Neuromuscul Disord. Sep-Nov;1993 3:423. [PubMed: 8186686]
34. Byrne BJ, Falk DJ, Clement N, Mah CS. Gene therapy approaches for lysosomal storage disease: next-generation treatment. Hum Gene Ther. Aug.2012 23:808. [PubMed: 22794786]
35. Lawlor MW, et al. Enzyme replacement therapy rescues weakness and improves muscle pathology in mice with X-linked myotubular myopathy. Human molecular genetics. Apr 15.2013 22:1525. [PubMed: 23307925]
36. Pierson CR, et al. Modeling the human MTM1 p.R69C mutation in murine Mtm1 results in exon 4 skipping and a less severe myotubular myopathy phenotype. Hum Mol Genet. Feb 15.2012 21:811. [PubMed: 22068590]
37. Mingozzi F, High KA. Immune responses to AAV vectors: overcoming barriers to successful gene therapy. Blood. Jul 4.2013 122:23. [PubMed: 23596044]
38. Hir ML, et al. AAV Genome Loss From Dystrophic Mouse Muscles During AAV-U7 snRNA-mediated Exon-skipping Therapy. Mol Ther. Jun 11.2013
39. Romero N. Centronuclear myopathies: a widening concept. Neuromuscul Disord. 2010; 20:223. [PubMed: 20181480]
40. Buchlis G, et al. Factor IX expression in skeletal muscle of a severe hemophilia B patient 10 years after AAV-mediated gene transfer. Blood. Mar 29.2012 119:3038. [PubMed: 22271447]
41. Smith RH, Levy JR, Kotin RM. A simplified baculovirus-AAV expression vector system coupled with one-step affinity purification yields high-titer rAAV stocks from insect cells. Mol Ther. Nov. 2009 17:1888. [PubMed: 19532142]
42. Petrov M, Malik A, Mead A, Bridges CR, Stedman HH. Gene transfer to muscle from the isolated regional circulation. Methods Mol Biol. 2011; 709:277. [PubMed: 21194035]
43. Carlson C, Makiejus R. A noninvasive procedure to detect muscle weakness in the mdx mouse. Muscle Nerve. 1990; 13:480. [PubMed: 2366821]
44. Goddard MA, Mitchell EL, Smith BK, Childers MK. Establishing clinical end points of respiratory function in large animals for clinical translation. Phys Med Rehabil Clin N Am. Feb.2012 23:75. [PubMed: 22239876]
45. Boutin S, et al. Prevalence of serum IgG and neutralizing factors against adeno-associated virus (AAV) types 1, 2, 5, 6, 8 and 9 in the healthy population: implications for gene therapy using AAV vectors. Hum Gene Ther. Jun.2010 21:704. [PubMed: 20095819]
46. Monteilhet V, et al. A 10 patient case report on the impact of plasmapheresis upon neutralizing factors against adeno-associated virus (AAV) types 1, 2, 6, and 8. Mol Ther. Nov.2011 19:2084. [PubMed: 21629225]

47. Skogstrand K, Multiplex assays of inflammatory markers. a description of methods and discussion of precautions - Our experience through the last ten years. Methods. Feb.2012 56:204. [PubMed: 22001645]

48. Malekzadeh A, et al. Challenges in multi-plex and mono-plex platforms for the discovery of inflammatory profiles in neurodegenerative diseases. Methods. Apr.2012 56:508. [PubMed: 22465283]

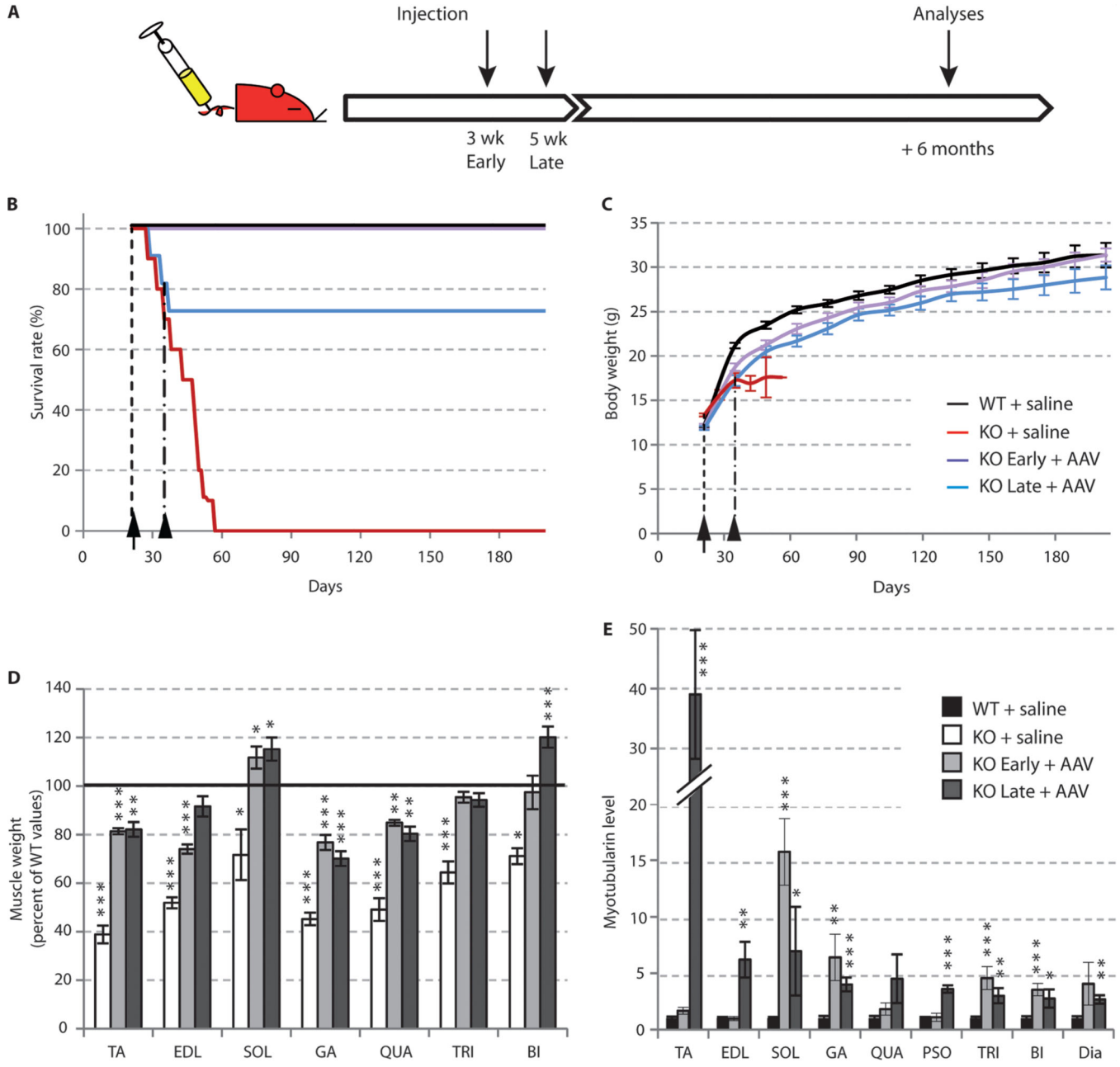

Figure 1.

Intravascular delivery of AAV8-*Mtm1* in myotubularin-deficient mice improves lifespan and body growth. **(A)** Experimental design. **(B)** Survival and **(C)** body mass of wild-type mice (WT) and constitutive KO-*Mtm1* mice injected at 3 weeks of age with saline (WT + saline, KO + saline, n=10 per genotype). Myotubularin-deficient mice were injected with AAV8-*Mtm1* at 3×10^{13} viral genomes per kg (vg/kg) at 3 (KO + AAV Early, n=8) and 5 weeks of age (KO Late + AAV, n=11) during a 6 months follow-up study. **(D)** Mass of representative skeletal muscles of KO-*Mtm1* mice 2 weeks after injection of saline (KO + saline, n=4) and 6 months (n=10 after injection of AAV8-*Mtm1* (KO Early + AAV, n=8, and KO Late + AAV, n=8). Values were normalized to muscle mass of age-matched, saline-injected WT

mice (n=10), taken as 100%. **(E)** Myotubularin protein quantification by immunoblot, GAPDH immunodetection was used an internal control. The number of animals was as in (C). Muscles: TA = tibialis anterior; EDL = extensor digitorum longus; SOL = soleus; GA = gastrocnemius; QUA = quadriceps; TRI = triceps; BI = biceps brachii; DIA = diaphragm. Statistical significance: $P < 0.05$ (one symbol); $P < 0.01$ (two symbols); $P < 0.001$ (three symbols); each condition versus WT + saline values.

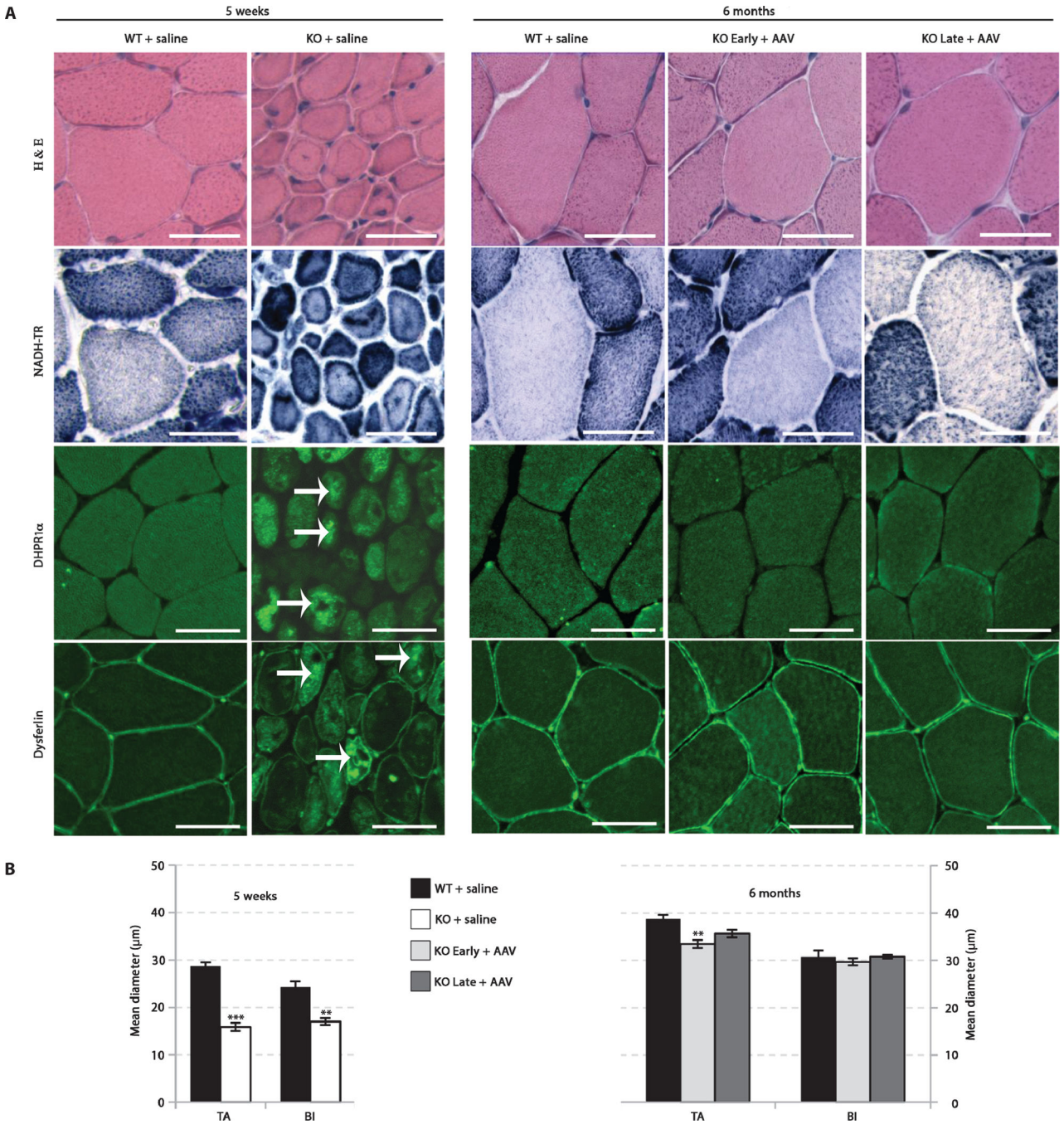

Figure 2.

Mtm1 gene replacement therapy corrects the internal architecture and hypotrophy of skeletal muscle fibers in myotubularin-knockout mice. Treatment groups were as described in Fig. 1. Mice were injected with either saline (+ saline) or AAV8-*Mtm1* vector (+ AAV). Sections were obtained after 2 weeks (5 weeks of age) and after 6 months of treatment. **(A)** Cross-sections from tibialis anterior (TA) muscle stained with hematoxylin and eosin (HE) and NADH-TR, and by immunofluorescence with antibodies against DHPR1α and dysferlin. Scale bars = 10 μm. **(B)** Mean diameter of muscle fibers from TA and biceps brachii

muscles from mice injected with either saline or AAV8-*Mtm1* after 2 weeks (left graph, WT + saline, n=10; KO + saline, n=4) and after 6 months of treatment (right graph, WT + saline, n=10; KO Early + AAV, n=7, and KO Late + AAV, n=8). Statistical significance: $P < 0.05$ (one symbol); $P < 0.01$ (two symbols); each condition versus WT + saline values.

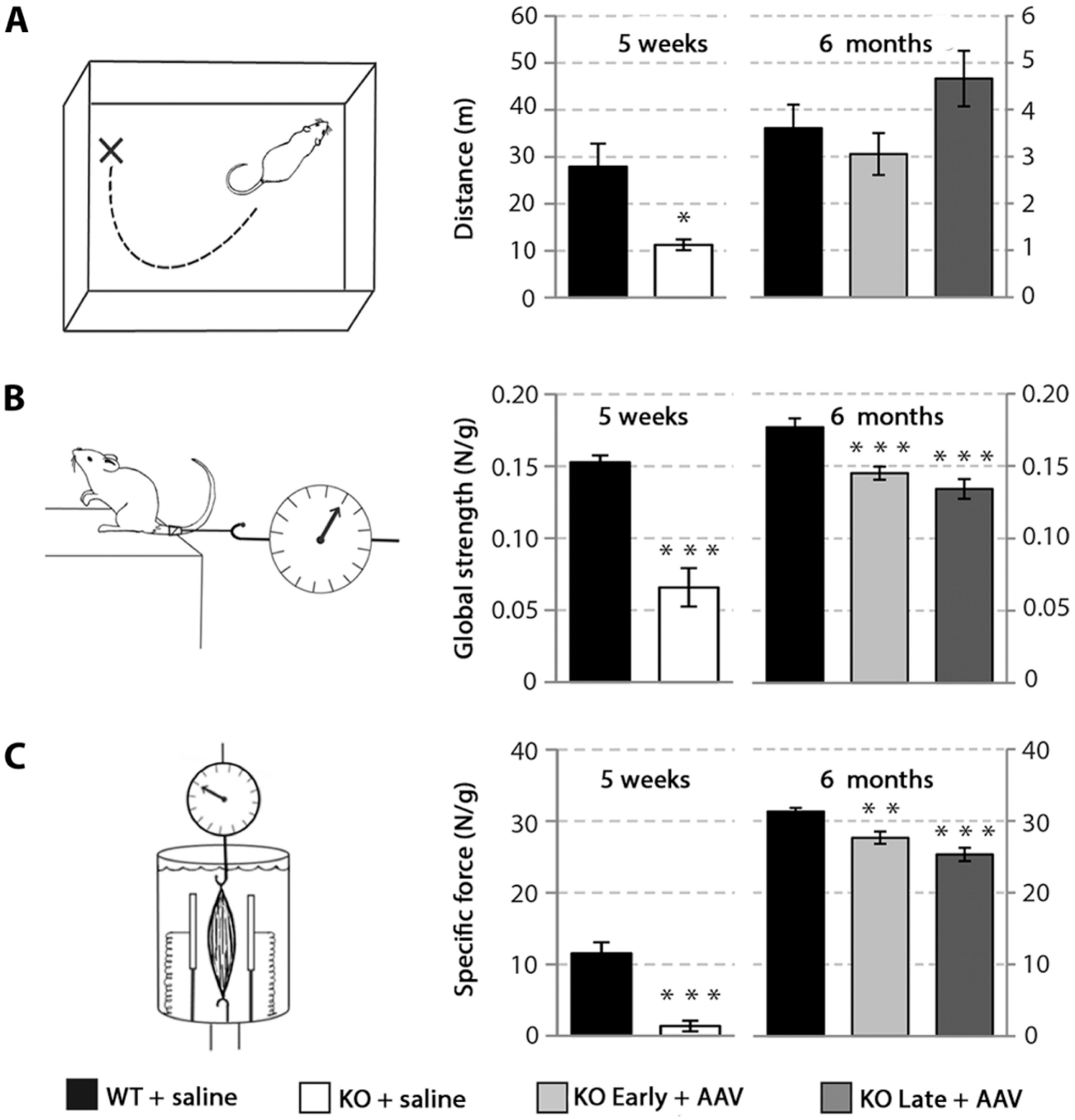

Figure 3.

Gene replacement therapy with AAV8-*Mtm1* improves strength, activity and long-term survival in myotubularin deficient mice. **(A)** Whole-body spontaneous mobility of normal (WT + saline), mutant (KO + saline) and AAV-treated mutant (KO Early and Late + AAV) mice, 2 weeks (5 weeks of age) and 6 months after PBS or vector injection. The distance covered over the 90-min test was assessed using an open field actimeter. **(B)** Escape test measurements in the 5 groups of mice. **(C)** Specific tetanic force of isolated EDL muscles from KO mice injected at an early and late stage of the disease 6 months after vector

delivery compared to saline-injected KO and WT littermates. Drawings of the tests are shown on the left side of each figure section. WT + saline, n=6 and KO + saline, n=4 at 5 weeks; WT + saline, n=10, KO Early + AAV, n=8, and KO Late + AAV, n=8 at 6 months. Symbols for statistical significance: same as in Fig. 1.

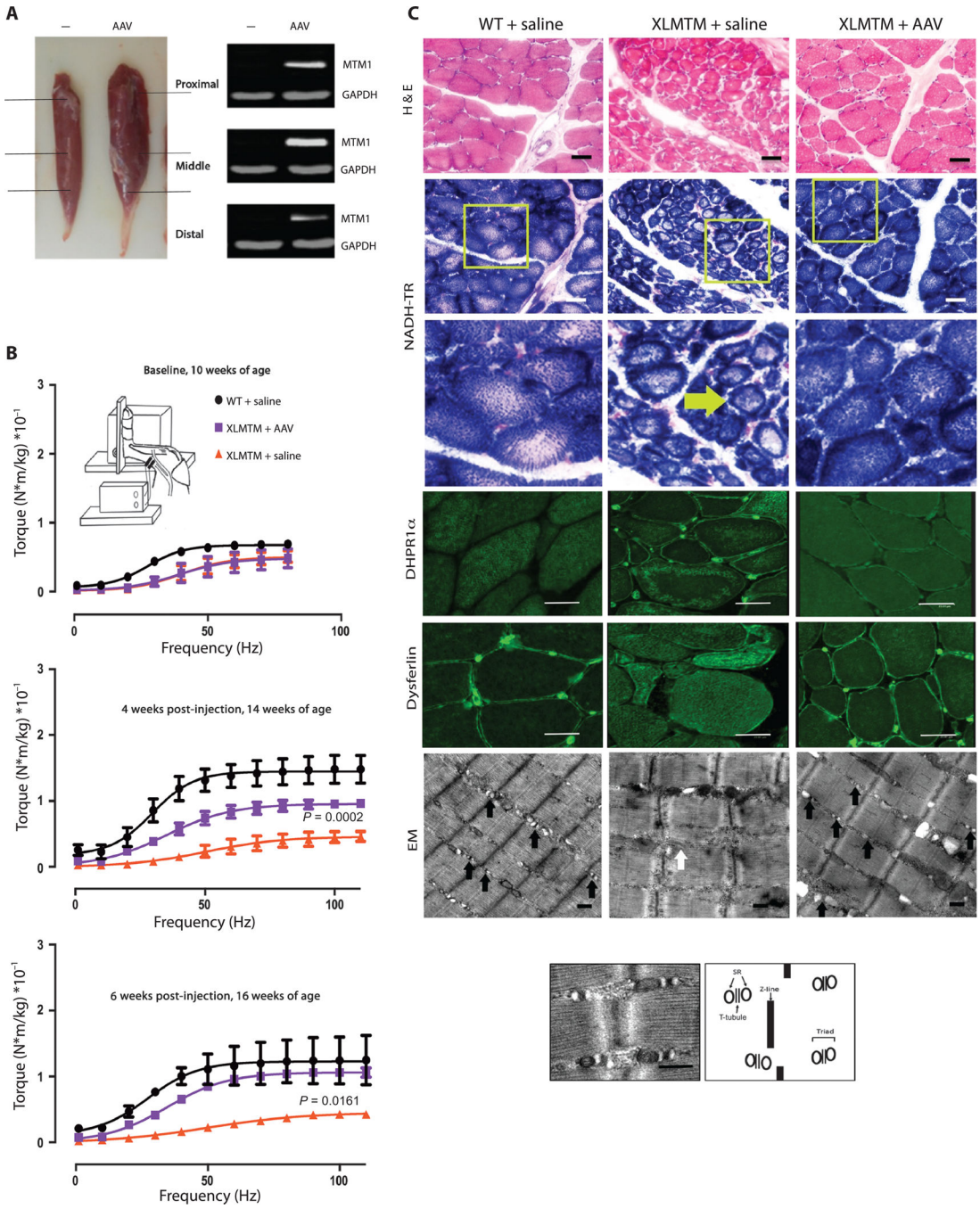

Figure 4.

Myotubularin is expressed and increases muscle mass and volume after local gene therapy in XLMTM dogs. (**A**) Cranial tibialis canine muscles 6 weeks post AAV8-MTM1 intramuscular injection. Immunoblot of myotubularin (MTM1, green) and GAPDH (red) from cranial tibialis muscle lysates at proximal (Prox), middle or distal section of the muscle. **(B)** MTM1 gene replacement therapy increases hind limb strength in XLMTM dogs. (Drawing) Method used to measure hind limb flexion strength in dogs. A nerve stimulator delivers electrical frequencies from 1-110 Hz to muscles that pull the paw toward

the stifle (knee). A transducer captures the torque generated when the paw pulls on the foot pedal. (Upper graph) Baseline prior to injection, 10 weeks of age (WT, n=3; XLMTM, n=3); (Middle graph) 4 weeks post-injection, 14 weeks of age (WT, n=3; XLMTM, n=3); (Bottom graph) 6 weeks post-injection, 16 weeks of age (WT, n=2; XLMTM, n=2). Symbols for statistical significance: same as in Fig. 1. **(C)** Local myotubularin gene replacement therapy improves muscle fiber architecture in XLMTM dogs. Cryosections of the cranial tibialis muscle (middle part) were assessed microscopically: boxes in NADH-TR staining show areas magnified below; immunofluorescence staining for DHPRα1 and dysferlin show correction of abnormal organelles with AAV8-MTM1. Size bars = 25 μm. Electron microscopy (EM) shows normal T-tubules (black arrows) and abnormal L-tubules (white arrow). Bar = 500 nm. Bottom panel: Close-up of WT muscle and schematic showing normal relationship of sarcomere ends (Z-line), and triads of T-tubles and sarcoplasmic reticulum (SR).

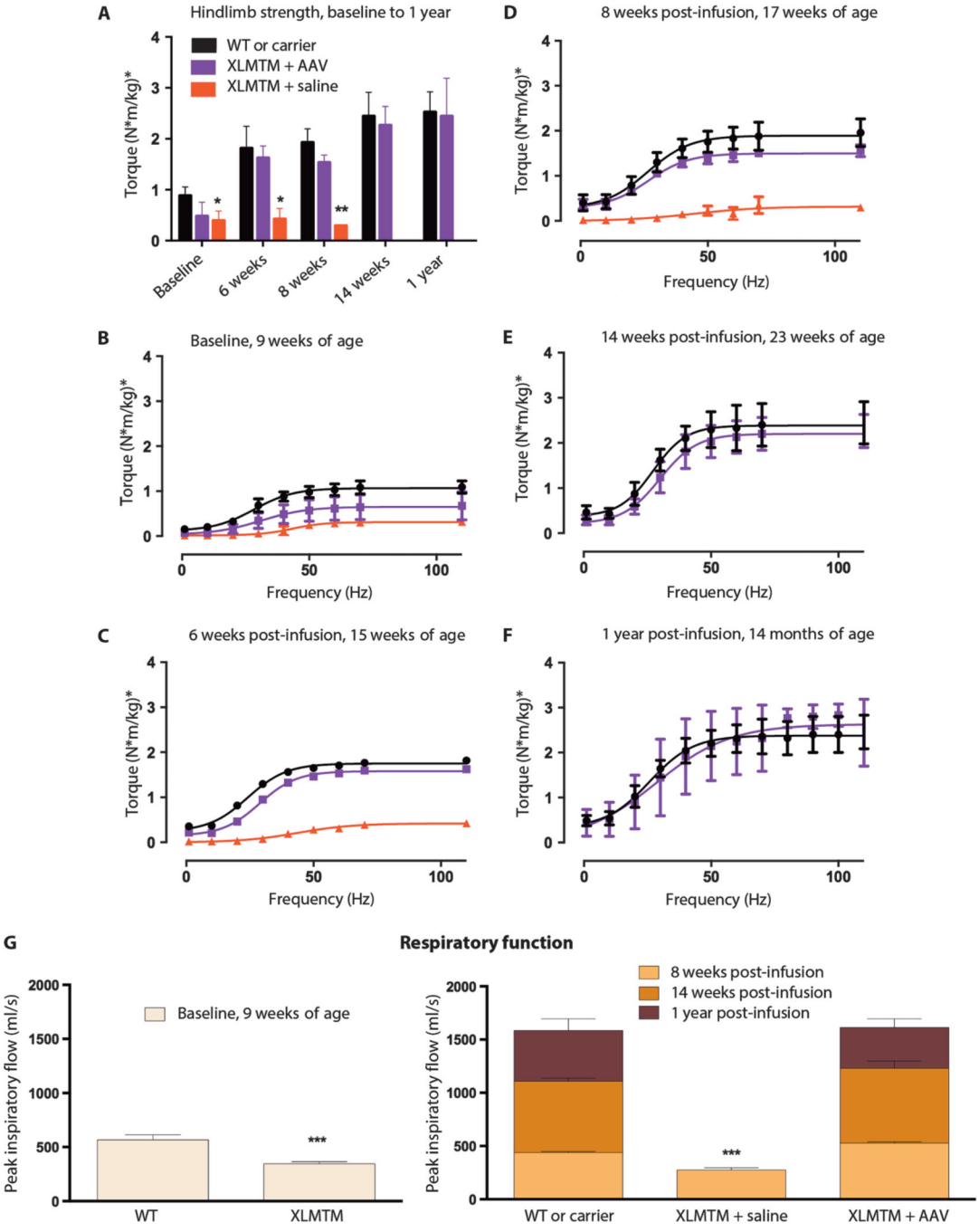

Figure 5.

(A-F) Hind limb strength of XLMTM dogs after intravascular administration of AAV8-*MTM1*. Data presented as mean ± SD combined values of both limbs. (**A**) Peak hind limb torque at various times up to 1 year after infusion. (**B**) Baseline prior to infusion, 9 weeks-of-age (WT, n=2; XLMTM + AAV8, n=3; XLMTM + Saline, n=1); (**C**) 6 weeks post-infusion, 15 weeks of age (WT, n=2; XLMTM + AAV8, n=2; XLMTM + Saline, n=2); (**D**) 8 weeks post-infusion, 17 weeks of age (WT, n=3; XLMTM + AAV8, n=3; XLMTM + Saline (n=3)); (**E**) 14 weeks post-infusion, 23 weeks of age (WT, n=3; XLMTM + AAV8,

n=3). Note: XLMTM dogs infused only with saline did not survive beyond 18 weeks of age. (**F**). One year post-infusion (WT, n=1, carrier, n=3, XLMTM + AAV8, n=3). (**G**) Peak inspiratory flow (PIF), a respiratory functional measure reflecting diaphragm muscle strength, taken in anesthetized dogs at baseline and at 8, 14 weeks and 1 year post infusion with AAV8. Number of animals/group: same as in b–f. Symbols for statistical significance: same as in Fig. 1.

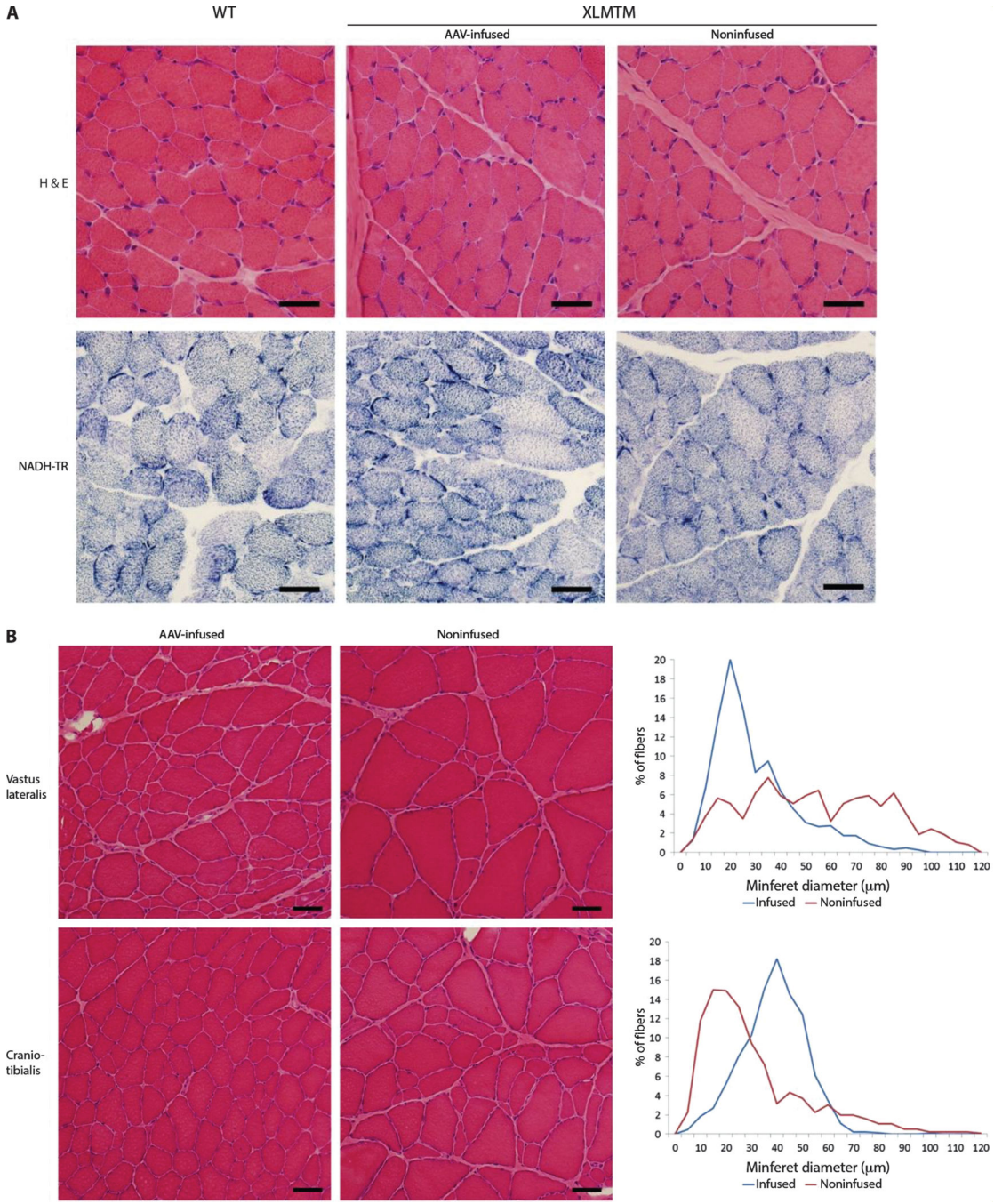

Figure 6.

MTM1 gene replacement therapy corrects the internal architecture and hypotrophy of skeletal muscle fibers in myotubularin-mutant dogs. Muscle cryosections from age-matched wild-type (WT) or rAAV8-MTM1 infused XLMTM dogs were assessed microscopically. Comparison is shown between the left (infused) hindlimb and the right (contralateral non-infused) limb. (**A**) Representative micrographs of HE and NADH-TR staining of quadriceps muscle cross-sections from muscle biopsies taken 4 weeks-post infusion from dog, “D4”.

(B) HE stained cranial tibialis cross-sections taken 1 year post AAV infusion. (Lower graph) myofiber diameter frequency distribution of images shown above. Size bars = 25 μm.

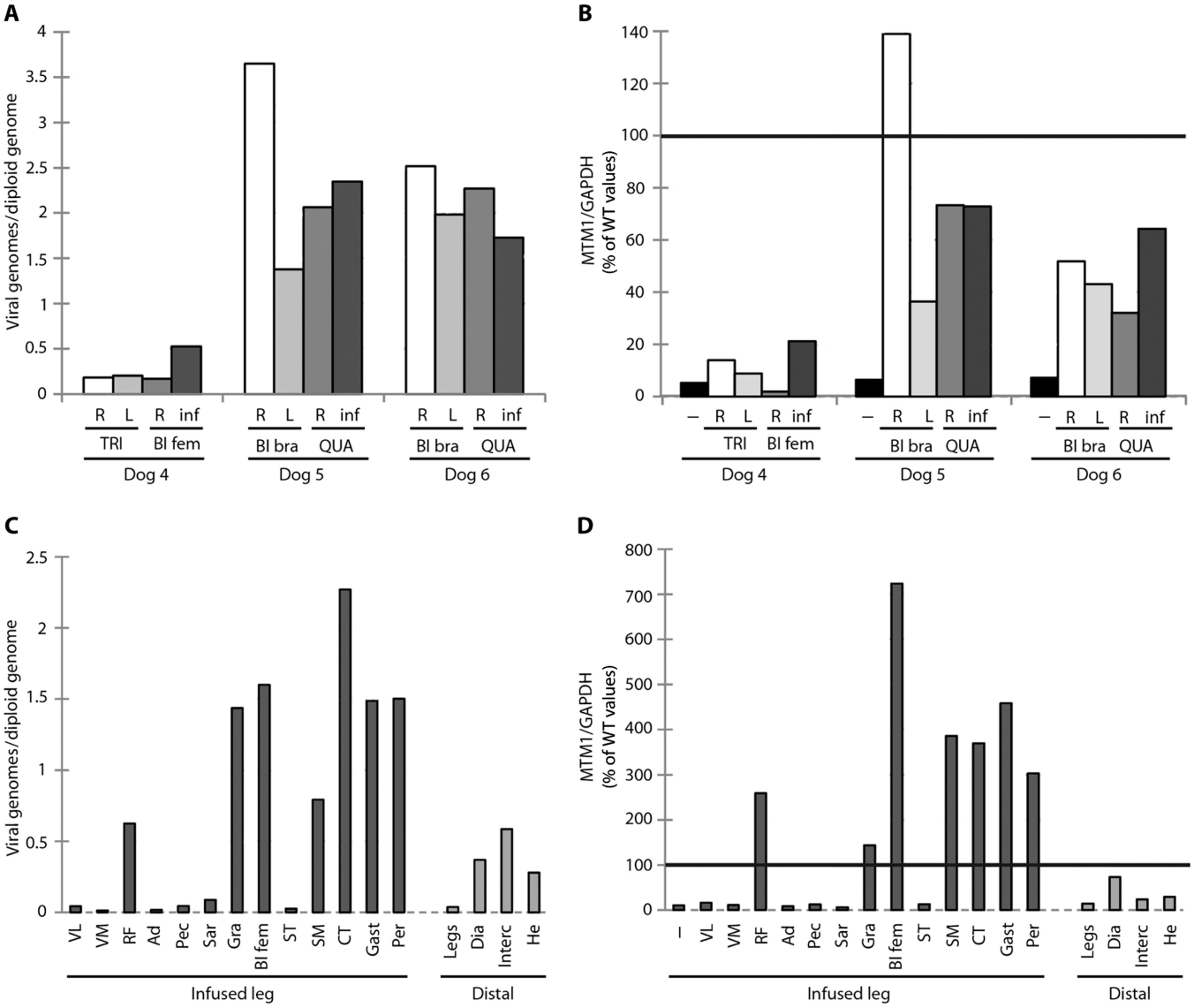

Figure 7.

Biodistribution of AAV8 vector and myotubularin transgene expression in XLMTM dogs infused with AAV8-MTM1. Comparison of vector distribution (A) and MTM1 transgene expression (B) among upper and lower limb muscle biopsies collected 4 weeks post-infusion in three XLMTM dogs, Dog 4, Dog 5 and Dog 6. Legend: Upper limb muscles: triceps, biceps brachii (TRI, BI bra, respectively). Lower limb muscles: biceps femoris, quadriceps (BI fem, QUA). R=right, L=left, inf = infused limb. (B) Expression of canine MTM1 protein relative to the housekeeping gene, GAPDH in whole muscle lysates probed with an anti-myotubularin antibody. Comparison of vector distribution (C) and MTM1 transgene expression (D) among upper and lower limb muscle necropsy samples collected 1 year post-infusion in D4, an XLMTM dog. Legend: muscles of the infused leg, VL=vastus lateralis; VM=vastus medialis; RF=rectus femoris; Ad=adductor magnus; Pec=pectineus; Sar=cranial Sartorius; Gra=gracilis; BI fem=biceps femoris; ST=semitendinosis; SM=semimembranosis;

CT=cranial tibialis; Gast=gastrocnemius; per=peroneus longus. Muscles distal to the infused leg, Dia=diaphragm, Interc=intercostals, He=heart.